The X-ray Absorption Spectra of Dissolved Polysulfides in Lithium – Sulfur Batteries from First Principles

Tod A. Pascal[a], Kevin H. Wujcik[b,c], Juan Velasco-Velez[d], Chenghao Wu[d], Alexander A. Teran[b,c], Mukes Kapilashrami[d], Jordi Cabana[b,c,e], Jinghua Guo[d], Miquel Salmeron[c], Nitash Balsara[b,c] and David Prendergast[a*]
[a]The Molecular Foundry, Materials Sciences Division, Lawrence Berkeley National Laboratory, Berkeley, California 94720, USA
[b]Department of Chemical and Biomolecular Engineering, University of California, Berkeley, California 94720, USA
[c]Environmental Energy Technologies Division, Lawrence Berkeley National Laboratory, Berkeley, California 94720, USA
[d]Advanced Light Source, Lawrence Berkeley National Laboratory, Berkeley, California 94720, USA
[e]Department of Chemistry, University of Illinois at Chicago, IL, 60605

Supporting Information

Computational Methodology

I) Description and preparation of solvated polysulfides

Optimized gas phase models of the lithium polysulfide species [Li_2S_x; x = 2 → 8] were obtained by energy minimization of a random starting structure using the Q-Chem 4.0 quantum chemistry package[1]. We employed the augmented polarized triple-ζ 6-311 +G(2d,2p) basis set of Pople and coworkers[2], a well balanced basis set that is a reasonable compromise between speed and accuracy. We inserted the optimized structures into a pre-equilibrated box of 12 TEGDME molecules, commonly used as a model solvent of polymeric electrolytes in lithium sulfur batteries[3,4]. After insertion, we removed any TEGDME molecules within 3Å of the polysulfide molecule. Generally, this leads to the elimination of 2 TEGDME molecules.

II) First-Principles Molecular Dynamics Simulations

The bulk TEGDME and the starting Li_2S_x-TEGDME systems were simulated using a modified version of the mixed Gaussian and plane wave code[5] CP2K/Quickstep[6]. We employed a triple-ζ basis set with two additional sets of polarization functions (TZV2P)[7] and a 320 Ry plane-wave cutoff. The unknown exchange-correlation potential is substituted by the PBE generalized gradient approximation[8] (consistent with our XAS simulations), and the Brillouin zone is sampled at the Γ-point only. Interactions between the valence electrons and the ionic cores are described by norm-conserving pseudopotentials[9,10]. The Poisson problem is tackled

using an efficient Wavelet-based solver[11]. We overcome the poor description of the short-range dispersive forces within the PBE-GGA exchange-correlation functional by employing the DFTD3 empirical corrections of Grimme et al.[12]. As a figure of merit, consider that cell dimensions from our pure TGEDME simulations in the constant pressure (1 bar), constant temperature (298 K) NPT ensemble were 1.66x1.92x1.10 nm^3, which gives a calculated density of 1.04 g/mL, in excellent agreement with the experimental value of ~1.0 g/mL[13].

In order to equilibrate the systems, we performed 10 ps of NPT dynamics, using a Nose-Hoover thermostat (temperature damping constant of 100 fs) and an Anderson barostat (pressure damping constant of 2 ps). Snapshots of the system were saved every step. The snapshot with a volume closest to the average of the last 5 ps of MD was then selected as input for an additional 20 ps simulation in the constant volume, constant temperature (canonical or NVT) ensemble. Snapshots of the system every 2 ps (for a total of 10 snapshots) were selected as input for first principles X-ray absorption calculations.

III) First-Principles DFT XCH calculations

All our XCH calculations employed the same periodic boundary conditions as our FPMD simulations, and used the PBE-GGA functional[8], and plane-wave pseudopotentials with a kinetic energy cutoff for the electronic wavefunctions (density) of 25 (200) Ry. Core-excited ultrasoft pseudopotentials and corresponding atomic orbitals were generated with the Vanderbilt code[14]. Matrix elements representing intensity of the core-excited excitations were evaluated within the projector-augmented-wave (PAW) frozen-core approximation[15]. The PWSCF code within the Quantum-Espresso package[16] was used to generate the core excited Kohn-Sham eigenspectrum, while the Shirley interpolation scheme[17] was used to accelerate numerical convergence of the computed spectra. The calculated XAS is taken as the statistical average of the spectrum of every sulfur atom in the structure, which includes intrinsic line shape broadening resulting from finite temperature effects at 298K, but we also include a 0.1 eV Gaussian convolution to guarantee a continuous spectral contribution from each atom. We verified that our spectra are insensitive to the choice of Gaussian broadening by repeating our calculations using 0.05, 0.2, 0.3, 0.4 and 0.5 eV Gaussians; the calculated spectra only changed in lineshape and peak ratios above 0.4 eV.

Due to the use of pseudopotentials in our calculations (which means that we can only reliably compare the relative calculated excitation energies), we have developed an alignment scheme based on formation energy differences between the ground and core-excited states of the system and those of an isolated atom in the same simulation cell[18,19]. Direct comparison to experiment is accomplished by first calibrating an unambiguous reference system. In the case of the sulfur compounds considered in this study, we rigidly shifted the first major peak in the sulfur K-edge XAS of an isolated S_2 molecule by +2467.5 eV to match the same in a gas phase experiment[20]. This empirical shift, is unique to the pseudopotentials employed in this study, and is applied to all subsequent calculated spectra. Previous experience has shown that this alignment scheme predicts XAS peak positions to within ~0.1 eV[19,21], which is typical of the experimental uncertainty in this energy range.

Our approach follows the Delta-Self-Consistent Field (ΔSCF) procedure to estimate the excitation energies. It is well know that Kohn-Sham DFT within the PBE approximation underestimates band gaps[22,23] and concomitantly band widths, due to inaccurate estimates of quasiparticle (excitation) energies based solely on the Kohn-Sham eigenspectrum[24,25]. As a result, the calculated XAS is usually too narrow with respect to the energy axis when compared to experiment. For example, in a previous study[21] we found that the band-gap of lithium fluoride, a rocksalt crystal, is underestimated by ~50% using PBE-DFT, and the resulting spectrum was contracted by 12% compared to experiment. In this study, we found that dilating the S_2 spectrum by 10% greatly improved agreement with experiment.

Validation of Computation Approach

The XCH approach has been shown accurate in reproducing the experimental K-edge XAS spectra of liquids[26,27] and of solids[18] and for interpreting the structure of various solvated organics and biomolecules[28,29]. We have recently validated our approach by comparing the calculation of lithium K-edge XAS to high resolution X-ray Raman spectroscopy measurements[21]. Within the context of the current study, we provide further validation by comparing the calculated sulfur K-edge XAS of crystalline elemental sulfur (αS_8) and Lithium sulfide (Li_2S) to experiment.

Applying the same rigid shift and dilation factor as for molecular S_2 leads to excellent agreement with experiment for solid elemental sulfur, S_8. In particular, the first and second peak positions (2472.6 and 2480.2 eV) are well reproduced. Sampling from a 298 K ab-initio molecular dynamics trajectory leads to a slightly broader XAS spectrum, as evident by the reduction in the intensity of the first peak in the MD spectrum relative to the static crystal spectrum. The FPMD sampled spectrum is also smoother than that of the static crystal. These effects are a manifestation of so called “thermal broadening”, although we note that both effects are a natural consequence of the instantaneous distortions in the crystal lattice that breaks the degeneracy of the p-like excited states[21]. Our approach generally underestimates the oscillator strength of excitations beyond the first main peak, possibly due to neglecting many-body excitations at higher energies.

Similar to S_8, we find excellent agreement between the experimental and calculated spectra of crystalline Li_2S (figure S1b). Indeed the ability to equally describe the spectrum of these two very different systems (the polar covalent crystal Li_2S and the molecular crystal S_8) from first principles underscores the robustness of our approach. The experimental spectrum is characterized by three main peaks at 2473.8, 2476.1 and 2484.0 eV, which are well reproduced by our XCH calculations using the experimental crystal structure: 2473.8, 2476.0 and 2484.1 eV respectively. The agreement with experiment improves when considering the XAS spectrum from snapshots obtained from our FPMD simulation. While the peak positions are identical to the static crystal case, finite temperature broadening leads to a shoulder between 2479.0 and 2479.6 eV in agreement with experiment, while the static crystal spectrum predicts a well-resolved peak at this energy. Additionally, a broadened spectrum due to finite temperature effects improves agreement of peak intensity ratios between the first and second peaks (0.89,0.72,0.70) and the first and third peaks (1.09,1.09,1.02) when comparing (experiment, finite temperature sampling, and the static crystal), respectively.

Tables

Table S1: Average valence electron populations (and standard deviations) on the various components of a dissolved Li_2S_x molecule in TEGDME from FPMD simulations as calculated by Bader analysis.

Li_2S_x	Terminal S		Internal S		Lithium		$<S_x^{2-}>$	$<Li_2S_x>$
	avg	±	avg	±	avg	±		
2	-0.845	0.076	-	-	0.910	0.096	-1.690	0.130
3	-0.735	0.029	-0.265	0.029	0.971	0.003	-2.265	-0.322
4	-0.686	0.032	-0.189	0.032	0.974	0.003	-2.207	-0.259
5	-0.670	0.060	-0.142	0.036	0.976	0.003	-2.047	-0.094
6	-0.658	0.050	-0.117	0.036	0.976	0.003	-2.015	-0.062
7	-0.643	0.044	-0.101	0.033	0.977	0.003	-1.993	-0.038
8	-0.627	0.053	-0.084	0.032	0.978	0.003	-1.926	0.031

Table S2: Average S - S bond lengths of S atoms from FPMD simulations obtained from the first maximum in the radial distribution function (figure S3).

Li_2S_x	Terminal S atoms		Internal S Atoms	
	avg	±	avg	±
2	2.045	0.030	-	-
3	2.049	0.031	2.049	0.031
4	2.058	0.032	2.056	0.032
5	2.061	0.029	2.062	0.030
6	2.064	0.029	2.067	0.029
7	2.066	0.028	2.067	0.029
8	2.063	0.030	2.067	0.030

Figures

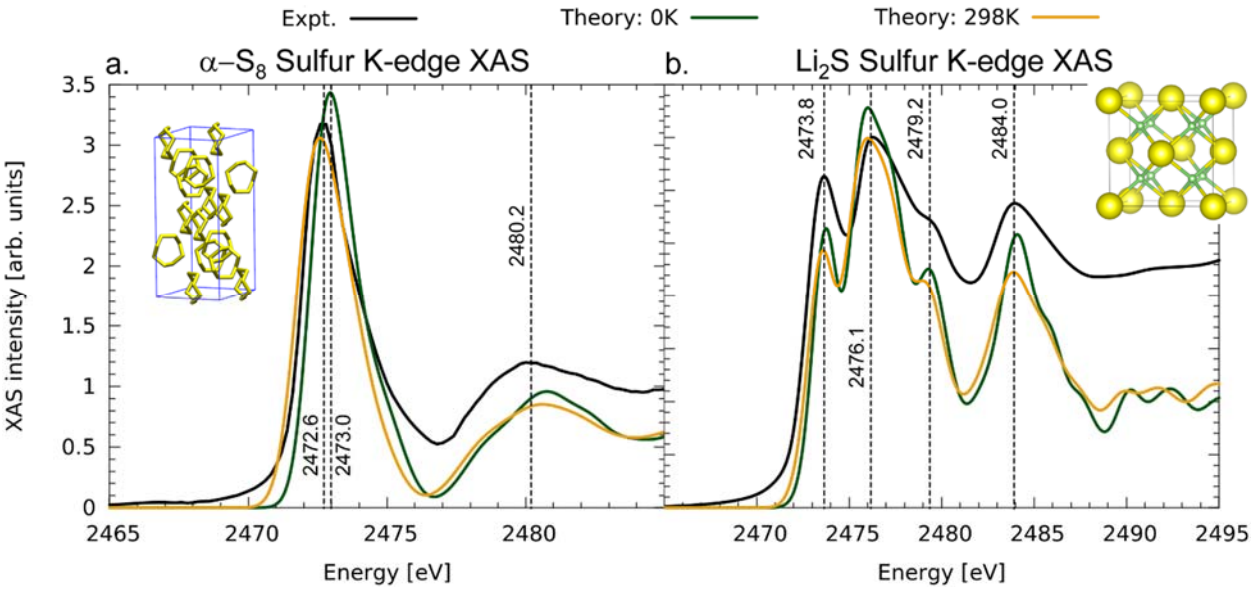

Figure S1: **(a)** Sulfur K-edge XAS spectra of elemental sulfur (rhombohedral αS_8). The experimental measurement[30] (black line), is compared to XCH-DFT calculations using the static crystal (green line) and ensemble structures from 298K first principles DFT simulations (gold line). The positions of the peak maximums are indicated by the dashed vertical lines. *Inset:* Crystal structure of αS_8 **(b)** Comparison of the Sulfur K-edge XAS spectra of crystalline Li_2S between experiment[31] and theory. The color scheme is the same as before. *Inset:* Crystal structure of Li_2S. The sulfur atoms (yellow spheres) and lithium atoms (green spheres) are indicated.

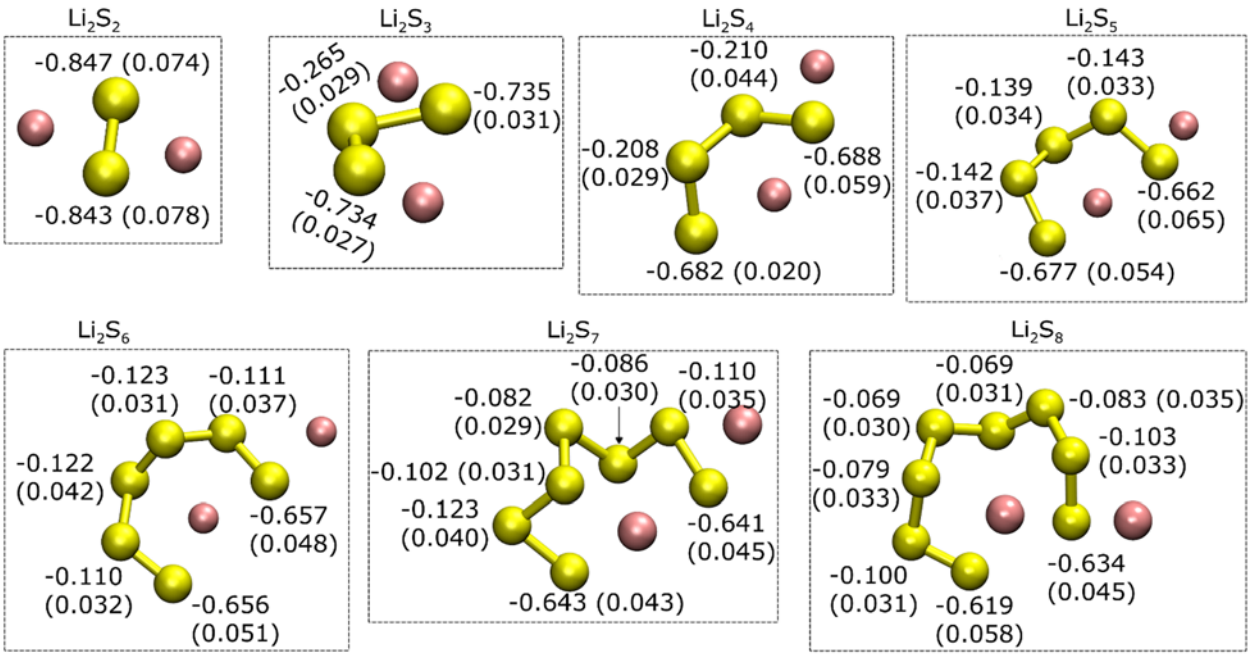

Figure S2: Average atomic charges of a Li_2S_x molecule dissolved in TEGDME from Bader analysis of an FPMD simulation. The molecular configuration shown has the highest population of the ensemble structures during the 25ps simulation. The TEGDME molecules are not shown for clarity. The charges on the Lithium atoms are not shown (see Table S1). The fluctuations (1σ) in the charges are indicated in the brackets.

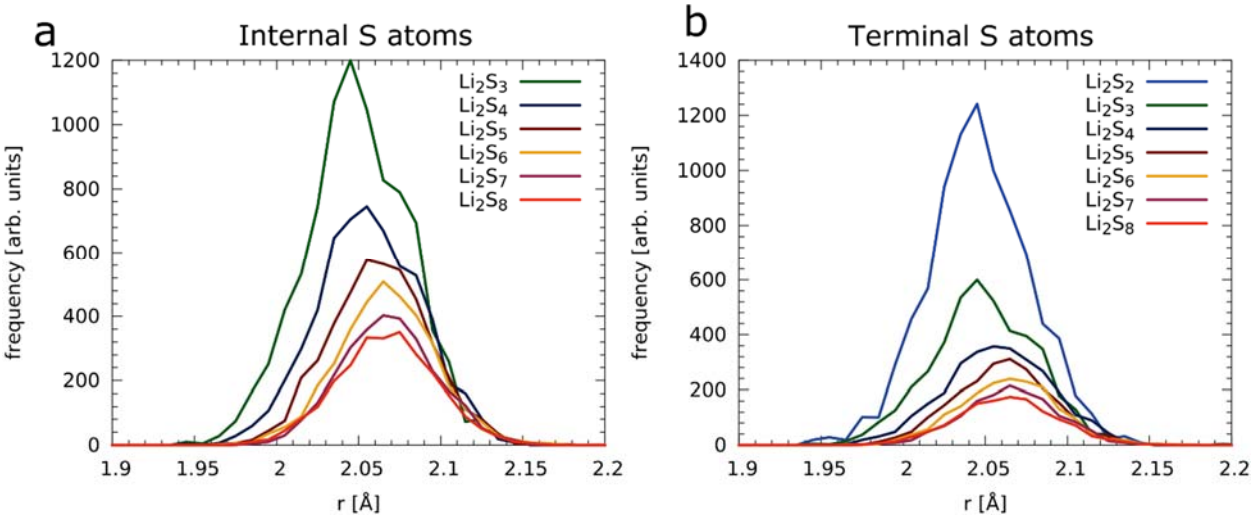

Figure S3: S - S bond distribution of (a) internal and (b) terminal Sulfur atoms of Li_2S_x from our first principles molecular dynamics simulations

References

(1) Shao, Y.; Molnar, L. F.; Jung, Y.; Kussmann, J.; Ochsenfeld, C.; Brown, S. T.; Gilbert, A. T.; Slipchenko, L. V.; Levchenko, S. V.; O'Neill, D. P. Advances in Methods and Algorithms in a Modern Quantum Chemistry Program Package. *Physical Chemistry Chemical Physics* **2006**, *8*, 3172-3191.

(2) Hehre, W. J. R., L.; Schleyer, P. v. R.; Pople, J. A.; *Ab Initio Molecular Orbital Theory*; Wiley: New York, 1986.

(3) Chang, D.-R.; Lee, S.-H.; Kim, S.-W.; Kim, H.-T. Binary Electrolyte Based on Tetra(Ethylene Glycol) Dimethyl Ether and 1,3-Dioxolane for Lithium–Sulfur Battery. *Journal of Power Sources* **2002**, *112*, 452-460.

(4) Gao, J.; Lowe, M. A.; Kiya, Y.; Abruna, H. D. Effects of Liquid Electrolytes on the Charge-Discharge Performance of Rechargeable Lithium/Sulfur Batteries: Electrochemical and in-Situ X-Ray Absorption Spectroscopic Studies. *J. Phys. Chem. C* **2011**.

(5) Lippert, G.; Hutter, J.; Parrinello, M. A Hybrid Gaussian and Plane Wave Density Functional Scheme. *Molecular Physics* **1997**, *92*, 477-487.

(6) VandeVondele, J.; Krack, M.; Mohamed, F.; Parrinello, M.; Chassaing, T.; Hutter, J. Quickstep: Fast and Accurate Density Functional Calculations Using a Mixed Gaussian and Plane Waves Approach. *Comput. Phys. Commun.* **2005**, *167*, 103-128.

(7) VandeVondele, J.; Hutter, J. Gaussian Basis Sets for Accurate Calculations on Molecular Systems in Gas and Condensed Phases. *J. Chem. Phys.* **2007**, *127*, -.

(8) Perdew, J. P.; Burke, K.; Ernzerhof, M. Generalized Gradient Approximation Made Simple. *Phys. Rev. Lett.* **1996**, *77*, 3865-3868.

(9) Goedecker, S.; Teter, M.; Hutter, J. Separable Dual-Space Gaussian Pseudopotentials. *Physical Review B* **1996**, *54*, 1703-1710.

(10) Krack, M. Pseudopotentials for H to Kr Optimized for Gradient-Corrected Exchange-Correlation Functionals. *Theor. Chem. Acc.* **2005**, *114*, 145-152.

(11) Genovese, L.; Deutsch, T.; Goedecker, S. Efficient and Accurate Three-Dimensional Poisson Solver for Surface Problems. *J. Chem. Phys.* **2007**, *127*, -.

(12) Grimme, S.; Antony, J.; Ehrlich, S.; Krieg, H. A Consistent and Accurate Ab Initio Parametrization of Density Functional Dispersion Correction (Dft-D) for the 94 Elements H-Pu. *The Journal of Chemical Physics* **2010**, *132*, 154104-154119.

(13) Hyun, J.-K.; Dong, H.; Rhodes, C. P.; Frech, R.; Wheeler, R. A. Molecular Dynamics Simulations and Spectroscopic Studies of Amorphous Tetraglyme (Ch3o(Ch2ch2o)4ch3) and Tetraglyme:Licf3so3 Structures. *The Journal of Physical Chemistry B* **2001**, *105*, 3329-3337.

(14) Vanderbilt, D. Soft Self-Consistent Pseudopotentials in a Generalized Eigenvalue Formalism. *Physical Review B* **1990**, *41*, 7892-7895.

(15) Taillefumier, M.; Cabaret, D.; Flank, A.-M.; Mauri, F. X-Ray Absorption near-Edge Structure Calculations with the Pseudopotentials: Application to the K Edge in Diamond and A-Quartz. *Physical Review B* **2002**, *66*, 195107.

(16) Giannozzi, P.; Baroni, S.; Bonini, N.; Calandra, M.; Car, R.; Cavazzoni, C.; Ceresoli, D.; Chiarotti, G. L.; Cococcioni, M.; Dabo, I. Quantum Espresso: A Modular and Open-Source Software Project for Quantum Simulations of Materials. *Journal of Physics: Condensed Matter* **2009**, *21*, 395502.

(17) Shirley, E. L. Optimal Basis Sets for Detailed Brillouin-Zone Integrations. *Physical Review B* **1996**, *54*, 16464.

(18) Jiang, P.; Prendergast, D.; Borondics, F.; Porsgaard, S.; Giovanetti, L.; Pach, E.; Newberg, J.; Bluhm, H.; Besenbacher, F.; Salmeron, M. Experimental and Theoretical Investigation of the Electronic

Structure of Cu[Sub 2]O and Cuo Thin Films on Cu(110) Using X-Ray Photoelectron and Absorption Spectroscopy. *The Journal of Chemical Physics* **2013**, *138*, 024704-024706.

(19) England, A. H.; Duffin, A. M.; Schwartz, C. P.; Uejio, J. S.; Prendergast, D.; Saykally, R. J. On the Hydration and Hydrolysis of Carbon Dioxide. *Chem. Phys. Lett.* **2011**, *514*, 187-195.

(20) Rühl, E.; Flesch, R.; Tappe, W.; Novikov, D.; Kosugi, N. Sulfur 1s Excitation of S2 and S8: Core–Valence- and Valence–Valence–Exchange Interaction and Geometry-Specific Transitions. *The Journal of Chemical Physics* **2002**, *116*, 3316-3322.

(21) Pascal, T. A.; Boesenberg, U.; Kostecki, R.; Richardson, T. J.; Weng, T.-C.; Sokaras, D.; Nordlund, D.; McDermott, E.; Moewes, A.; Cabana, J.; Prendergast, D. Finite Temperature Effects on the X-Ray Absorption Spectra of Lithium Compounds: First-Principles Interpretation of X-Ray Raman Measurements. *The Journal of Chemical Physics* **2014**, *140*, 034107-034121.

(22) Cohen, A. J.; Mori-Sanchez, P.; Yang, W. T. Fractional Charge Perspective on the Band Gap in Density-Functional Theory. *Physical Review B* **2008**, *77*.

(23) Mori-Sanchez, P.; Cohen, A. J.; Yang, W. T. Localization and Delocalization Errors in Density Functional Theory and Implications for Band-Gap Prediction. *Phys. Rev. Lett.* **2008**, *100*.

(24) Fuchs, F.; Furthmüller, J.; Bechstedt, F.; Shishkin, M.; Kresse, G. Quasiparticle Band Structure Based on a Generalized Kohn-Sham Scheme. *Physical Review B* **2007**, *76*, 115109.

(25) Aulbur, W. G.; Jonsson, L.; Wilkins, J. W. Quasiparticle Calculations in Solids. *Solid State Phys* **2000**, *54*, 1-218.

(26) Prendergast, D.; Grossman, J. C.; Galli, G. The Electronic Structure of Liquid Water within Density-Functional Theory. *J. Chem. Phys.* **2005**, *123*.

(27) Prendergast, D.; Galli, G. X-Ray Absorption Spectra of Water from First Principles Calculations. *Phys. Rev. Lett.* **2006**, *96*, 215502.

(28) Uejio, J. S.; Schwartz, C. P.; Duffin, A. M.; England, A.; Prendergast, D.; Saykally, R. J. Monopeptide Versus Monopeptoid: Insights on Structure and Hydration of Aqueous Alanine and Sarcosine Via X-Ray Absorption Spectroscopy. *J. Phys. Chem. B* **2010**, *114*, 4702-4709.

(29) Schwartz, C. P.; Uejio, J. S.; Duffin, A. M.; England, A. H.; Kelly, D. N.; Prendergast, D.; Saykally, R. J. Investigation of Protein Conformation and Interactions with Salts Via X-Ray Absorption Spectroscopy. *Proc. Natl. Acad. Sci. U. S. A.* **2010**, *107*, 14008-14013.

(30) Durand, J. M.; OlivierFourcade, J.; Jumas, J. C.; Womes, M.; Teodorescu, C. M.; Elafif, A.; Esteva, J. M.; Karnatak, R. C. K Edge Absorption Spectra of Sulphur in Vapour, Molecular and Polymerized Solid Phases. *Journal of Physics B-Atomic Molecular and Optical Physics* **1996**, *29*, 5773-5784.

(31) Cuisinier, M.; Cabelguen, P.-E.; Evers, S.; He, G.; Kolbeck, M.; Garsuch, A.; Bolin, T.; Balasubramanian, M.; Nazar, L. F. Sulfur Speciation in Li–S Batteries Determined by Operando X-Ray Absorption Spectroscopy. *The Journal of Physical Chemistry Letters* **2013**, *4*, 3227-3232.